Princeton Plasma Physics Laboratory

PPPL- 4413

PPPL- 4413

Non-Axisymmetric Shaping of Tokamaks Preserving Quasi-Axisymmetry

Long-Poe Ku and Allen H. Boozer

May, 2009

Prepared for the U.S. Department of Energy under Contract DE-AC02-09CH11466.

Non-Axisymmetric Shaping of Tokamaks Preserving Quasi-Axisymmetry

Long-Poe Ku
Princeton Plasma Physics Laboratory, Princeton University, Princeton, NJ 08543, lpku@pppl.gov
Allen H. Boozer
Columbia University, New York, NY 10027, ahb17@columbia.edu
(Dated: May 28, 2009)

If quasi-axisymmetry is preserved, non-axisymmetric shaping can be used to design tokamaks that do not require current drive, are resilient to disruptions, and have robust plasma stability without feedback. Suggestions for addressing the critical issues of tokamaks can only be validated when presented with sufficient specificity that validating experiments can be designed. The purpose of this paper is provide that specificity for non-axisymmetric shaping. To our knowledge, no other suggestions for the solution of a number of tokamak issues, such as disruptions, have reached this level of specificity. Sequences of three-field-period quasi-axisymmetric plasmas are studied. These sequences address the questions: (1) What can be achieved at various levels of non-axisymmetric shaping? (2) What simplifications to the coils can be achieved by going to a larger aspect ratio? (3) What range of shaping can be achieved in a single experimental facility? The sequences of plasmas found in this study provide a set of interesting and potentially important configurations.

I. INTRODUCTION

Stellarators, such as Wendelstein 7AS (W7AS) and the Large Helical Device (LHD), which have strong non-axisymmetric shaping, have yielded impressive performance [1], [2]. The experiments have found stable high volume-averaged beta, $\beta \equiv \langle 2\mu_0 p/B^2 \rangle$ plasmas that last hundreds of energy confinement times [6], high density ($\geq 10^{21}/m^3$) regimes exceeding the Greenwald density limit of tokamaks [7], and a scaling of confinement comparable to that of H-mode tokamaks [8]. These achievements coupled with the observed robust stability [1] without disruptive plasma terminations show that three-dimensional shaping of fusion plasmas addresses important issues that must be addressed before fusion power systems can be a reality.

Issues beyond those that will be addressed on the International Thermonuclear Experimental Reactor (ITER) [3] that must be addressed to make fusion power a reality were the subject of the report to the Fusion Energy Sciences Advisory Committee (FESAC) [4]. That report and the subsequent discussions imply that:

- A fusion plasma can have little external power input.

  A fusion power plant must generate far more power than it uses. Two implications are: (1) The control of a fusion plasma must be carried out with little power input. (2) The pressure and bootstrap current profiles are essentially self-determined by power balance between the fusion burn and the microturblent transport. The self-determination of plasma profiles is made even stronger by the absence of an accepted method of injecting particles into the center of a fusion plasma.

- Disruptions cannot be tolerated at any significant level in a fusion plasma.

  At present there is no accepted method of avoiding tokamak disruptions–even with far more complete diagnostics than are expected in a fusing plasma and even with controls that inject power equal to the total power that flows through the plasma.

- Feedback systems in fusion plasmas will be highly constrained.

  Each feedback system requires a diagnostic, but few diagnostics can withstand fusion conditions. The feedback control can require little power. The shielding of control coils will constrain the rapidity with which external magnetic fields can be changed.

- A close coupling between central plasma and edge plasma conditions makes extrapolations to fusion conditions difficult and endangers plasma facing components

  In high performance tokamaks, the central temperature is empirically found to be determined by the conditions on the inner side of the edge pedestal region, which is sensitive to wall conditions. This feature of the central temperature is theoretically understood as a result of the critical-gradient nature of Ion Temperature Gradient (ITG) microturbulence. A consequence is that a sudden change in the pedestal plasma, such as Edge Localized Modes (ELMs), can deposit a significant fraction of the plasma energy on divertor components, which gives an unacceptable rate of erosion. Even if ELMs are avoided, the high edge temperature and the low edge density, which are characteristic of tokamaks operating at the critical gradient, makes it difficult to have an acceptable strategy for ensuring the survivability of the chamber walls and the divertor.

  Wall conditions will be very different in a fusion plasma than in ITER. In ITER, as in existing tokamaks, the walls are much colder than in a fusion system. Hot walls, unlike those in existing experiments, generally reflect particles. Liquid lithium, which requires a relatively low wall temperature not to evaporate, can give an absorbing boundary condition for particles, which also differs from that in present experiments.

To achieve the programmatic mission of ITER, which is "*to demonstrate the scientific and technological feasibility of fusion power for peaceful purposes,*" these issues imply that it is necessary to

- Provide sufficient poloidal magnetic field to ensure the maintenance of the magnetic configuration and to allow compensation for the uncertainty or mismatch in the profile of the bootstrap current.

  In the physics basis of ITER, it was concluded [5] that the part of the poloidal field produced by external current drive in ITER will be four times larger than that allowable in a demonstration of fusion power (DEMO). ITER is not expected to fully test either the maintenance or the control of poloidal field profile at the level required for DEMO. It should also be noted that even low levels of external current drive place great demands on the development of suitable external sources [4].

- Ensure sufficiently robust plasma stability to prevent disruptions.

- Minimize the need for feedback systems.

- Maintain a large center to edge ratio in the ion temperature and a high plasma density.

Since fusion plasmas are in a self-organized state, the primary design freedom to meet these requirements is non-axisymmetric shaping [9], [10]. Axisymmetric tokamaks have a space of only about four shaping parameters, which are aspect ratio, ellipticity, triangularity, and squareness. This space can be expanded to about forty parameters if non-axisymmetry is allowed. The empirical studies of non-axisymmetric shaping have been in stellarator experiments, which differ greatly from the extensively studied axisymmetric tokamak in having strong asymmetries in the magnetic field strength and sufficiently strong shaping to produce most of the poloidal magnetic field. A clear need exists to understand the benefits of shaping on magnetically confined plasmas that lie between axisymmetric tokamaks and stellarators.

The extension of the design space of tokamaks by non-axisymmetric shaping depends on the concept of quasi-axisymmetry (QA). A magnetic field satisfies the constraint of quasi-symmetry if the field lines lie in nested toroidal surfaces, called magnetic surfaces, and the magnetic field strength along each field line obeys $B(\ell) = B(\ell + L)$, where ℓ is the distance along the line and L is a constant along that line [9]. Quasi-symmetric systems can either extend the space of axisymmetry or helical symmetry. The principles of quasi-symmetry have been demonstrated in the Helically Symmetric Experiment (HSX) [11]. However, quasi-axisymmetry has not been studied in an experiment other than near the axisymmetric limit, $\delta B/B \lesssim 10^{-3}$.

Theoretical and numerical investigations of QA stellarators were pioneered by Nührenberg and Garabedian [12], [13], [14], and the potential of a quasi-axisymmetric stellarator as a fusion power reactor has been studied [15]. An experimental device [16], the National Compact Stellarator Experiment (NCSX), was proposed in the late 1990's, but the construction was terminated in 2008 during the final stages of manufacture and assembly. These studies have demonstrated the existence of a wealth of available QA configurations. Nevertheless, most of these configurations were constructed and optimized only to meet the objectives of each individual study. The breadth of shaping options that exist for quasi-axisymmetric stellarators has not been examined systematically.

No experiments have been performed in which quasi-axisymmetry was preserved while breaking axisymmetry at a level above $\delta B/B \sim 10^{-3}$. Nevertheless, the commonality of the physics, the design tools, and the extensive experimental data base of stellarators allow the design of tokamak-like magnetic configurations that address issues that must be addressed to make fusion a reality. This paper demonstrates the existence of sequences of QA configurations that can be constructed with various levels of externally supplied poloidal magnetic field over a wide range of aspect ratios. These sequences clarify the benefits that can be obtained at various levels of shaping. The paper also shows that it is in principle possible to construct a single device that would enable an empirical study of a broad sequence of QA configurations.

Suggestions for addressing the critical issues of tokamaks can only be validated when presented with sufficient specificity that validating experiments can be designed. The purpose of this paper is provide that specificity for non-axisymmetric shaping. To our knowledge, no other suggestions for the solution of a number of tokamak issues, such as disruptions, have reached this level of specificity.

Section (II) briefly discusses the approach and methods used in the investigation. Section (III) shows configurations with weak, moderate, and strong shaping, which illustrate attainable plasma control. Section (IV) examines the effect of the toroidal aspect ratio on the complexity of the coils. Section (V) gives a design using a combination of trim and planar toroidal field coils to realize a sequence of plasmas with various degrees of external shaping. Section (VI) gives a summary and the conclusions.

We note that the configuration space is rich and vast. It is not the purpose of this paper to identify the optimum QA configuration but to demonstrate the existence of QA configurations that could fundamentally change the perceived constraints of tokamak-like systems.

II. APPROACH AND METHODS

The plasma boundaries in the study are given in the Garabedian representation [17],

$$R + iZ = e^{iu} \sum_{mn} \Delta_{mn} e^{-imu+inv}, \qquad (1)$$

where R and Z are the radial and the axial components of (R, φ, Z) cylindrical coordinates, m and n are the poloidal and toroidal mode numbers, and u is a poloidal angle. The toroidal angle is $v = N_p\varphi$, where N_p is the number of toroidal periods of the shaping. The coefficient Δ_{00} is a measure of the plasma minor radius, and Δ_{10} the major radius. The elongation and triangularity in the plasma shaping are described by the $m = 2$, and 3 terms, respectively. The $\Delta_{1,n}$ terms give the helical excursion of the boundary.

Basic physics properties of a stellarator are determined once an outer magnetic surface is prescribed. The objective of this study is to optimize the boundary shape of configurations, which means the Δ_{mn}'s of Eq. (1), for providing a prescribed rotational transform, stabilizing the resistive wall modes (RWM's) at a prescribed plasma pressure, and adequately satisfying the quasi-axisymmetry requirement. The rotational transform $\iota \equiv 1/q$ is the average number of poloidal circuits a magnetic field line makes per toroidal circuit of the torus. An RWM is an ideal magnetohydrodynamic (MHD) plasma instability, called a kink mode, which would be stabilized if the structures surrounding the plasma had zero resistivity. There may be other requirements as well, such as the global shear in the rotational transform, the depth of magnetic well provided by the external shaping, *etc.*, which can be combined with the basic requirements to form an overall objective function. The configurations discussed in the following sections have been obtained in this fashion. They represent configurations that satisfy minimum requirements. In the landscape of the configuration space, they may be regarded as a local minimum of an objective function. Other configurations with different combinations of Δ_{mn}'s may exist that give a lower minimum of the objective function and are therefore better. This study was not designed to find either the global minimum or the best configuration but to show configurations exist that are sufficiently attractive that they demonstrate the importance of the quasi-axisymmetric shaping extension of the design space of tokamaks.

For some of the configurations, solutions for the required coils were found in order to study the issue of coil complexity. A simple approach was taken. A coil winding surface was chosen, which was typically conformal to the plasma surface shape but displaced from the plasma by a fixed amount. A solution was sought for the current potential κ such that the total normal field on the plasma surface was minimized in a root-mean-square sense. The normal field would be zero if the current potential produced the fields required to support a plasma with the precise shape that was prescribed. The surface current $\vec{K}$ of electrodynamics texts has the form $\vec{K} = \vec{\nabla}\kappa \times \hat{n}$, where $\hat{n}$ is the unit normal to the surface. The required coils are constant κ contours with the coil currents given by the change in κ between the coils. There are other more involved ways of designing stellarator coils, for example [18], but they do not provide additional insights for the study given in this paper.

The equilibria were obtained using the VMEC code [19], either in the fixed-boundary mode while finding optimal shapes, the Δ_{mn}'s, or in the free-boundary mode while investigating issues related to coils. In most cases the number of poloidal and toroidal harmonics was limited to no more than four in the Δ_{mn}'s, which corresponds to squareness for the highest poloidal shaping. External kink modes were analyzed using the three-dimensional ideal MHD code Terpsichore [20], which determines the growth rate of the unstable modes by minimizing the plasma potential energy. The measure of quasi-axisymmetry was based on the evaluation of helical ripples along field lines on a few flux surfaces using the NEO code [21] and by a direct examination of the magnetic spectrum in magnetic coordinates [22]. The design of the coils used a modified version of Merkel's NESCOIL code [23].

The calculations were carried out with a numerical resolution sufficiently fine that they should yield correct physics solutions, but not so fine as to render computations prohibitively expensive. For example, 49 flux magnetic surfaces were consistently retained in the equilibrium solutions and 91 selected perturbation modes in the stability calculations. The plasma pressure and bootstrap current profiles were taken from NCSX [24] but adjusted to obtained a fixed $\beta = 4\%$ and to reflect changes in the aspect ratio and the level of rotational transform, which means a correction for $R \cdot B_t$ and the trapped particle fraction.

III. CONFIGURATIONS WITH INCREASING LEVELS OF ROTATIONAL TRANSFORM

This section considers two sequences of quasi-axisymmetric (QA) configurations: one with weak to moderate shaping, which illustrates the benefits of various levels of shaping, and one with stronger shaping, which shows the difference between distinct sequences of QA configurations. All of the configurations discussed in this section have three periods, $N_p = 3$, and an aspect ratio, $A \approx 4$.

Figure (1) shows configurations with the externally provided rotational transform ranging from 0.05 to 0.30, which accounts for about $20-60\%$ of the total rotational transform at 4% beta. These configurations have similar shapes. The toroidally averaged elongation is ≈ 1.8. The rotational transform was mostly produced by the Δ_{21} term in Eq. (1), which gives an ellipse with an orientation that rotates through a toroidal period. The Δ_{21} term is sufficiently small that a reasonable width is ob-

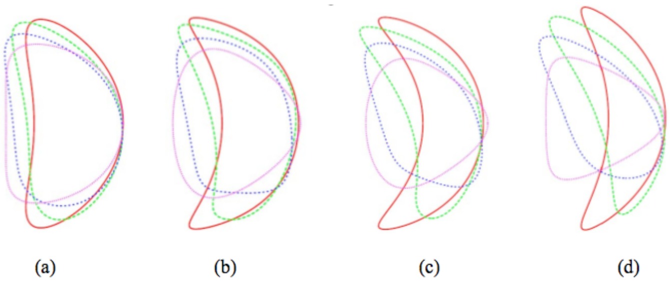

FIG. 1: Quasi-axisymmetric configurations with the rotational transform provided by the three-dimensional shaping in (a): 0.05, (b): 0.10, (c): 0.20 and (d): 0.30, shown in four cross sections with equally spaced toroidal angles over half period. Configuration (a) is passively stable to the vertical mode, (b) removes the need for current drive at $\beta = 4\%$, (c) remains in vacuum chamber if plasma pressure and current vanish instantaneously, and (d) is passively stable to the wall mode.

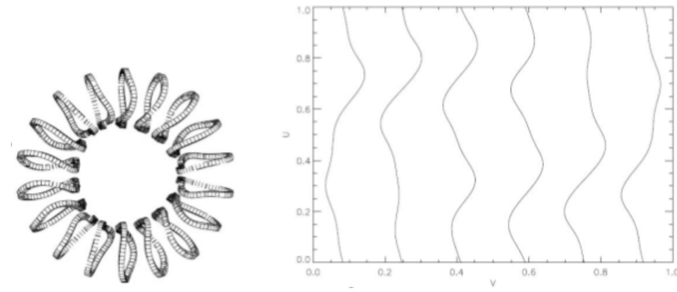

FIG. 2: A modular coil set designed for the configuration shown in Figure (1.a) with the current winding surface conformal to the boundary of the plasma and displaced outward by a distance equal to $0.6a$, where a is the average minor radius of the plasma. The left frame shows the coils, six per field period, viewed from the top. The right frame shows the contours of current potential on the flattened winding surface in one field period with the abscissa being the toroidal angle, v, and the ordinate the poloidal angle, u. The toroidal angle starts at the crescent-shaped cross section and the poloidal angle starts at the outboard mid-plane.

tained in the crescent-shaped cross section.

The construction was also designed to increase the overlapping volumes of the non-axisymmetric and the underlying axisymmetric configuration with an eye towards designing a device capable of performing experiments from a tokamak to a QA stellarator.

The configurations were designed to have a magnetic well of 2-3% in the absence of the plasma pressure. Although ballooning stability was not specifically targeted in the optimization of the boundary shape, the configurations have reasonably good ballooning stability characteristics. A large plasma current increases the shear in the core region, which improves the kink stability. Quasi-axisymmetry was targeted using helical ripple as a measure, which meant ϵ_{eff} [21] was less than 1% in the bulk of the plasma. In practice, we were able to achieve the quasi-axisymmetry much better, typically $\epsilon_{eff} < 0.7\%$ in the core region. The residues in the magnetic spectrum, $n \neq 0$, were kept below a few percent relative to the field strength on the magnetic axis.

The configuration with the lowest transform, Figure (1.a), was targeted to be passively stable to the vertical mode, which means $(m = 1, n = 0)$ as well as other modes that the plasma shaping linearly couples to it, such as $m = 8, n = 3$. The modes that are linearly coupled to an $n = 0$ perturbation are called an $N = 0$ family of perturbations. No penalty was taken in the optimization for instabilities of the $N \neq 0$ families. The amount of external transform needed to stabilize the vertical mode depends on the toroidally averaged elongation. The configuration shown has an averaged elongation of 1.8. This is an elongation that is typical of modern tokamaks, but in axisymmetry feedback stabilization is required. The required external transform, ≈ 0.05, to passively stabilize the vertical instability is smaller but generally consistent with a formula that was derived by Fu [25] assuming a large aspect ratio and a flat rotational transform. The deformation of the plasma is modest and can be produced by moderately deforming the planar toroidal field coils, as illustrated in Figure (2), or by using trim coils in conjunction with planar toroidal and poloidal field coils. For this case, the external transform is not sufficient to have robust plasmas at high beta without current in the plasma core in addition to the bootstrap current. An additional current was assumed, which raised the central iota to $\iota \approx 0.33$, which is a safety factor $q \equiv 1/\iota \approx 3$.

To avoid the need for current drive, the externally provided transform must be increased, as in the example shown in Figure (1.b), which has an external rotational transform of ≈ 0.1. The safety factor $q = 1/\iota$ at the magnetic axis is about 20, but ι increases rapidly away from the axis due to the bootstrap current. The shift of the magnetic axis at 4% beta is about 35% of the average minor radius a, which is defined so $B_0 \pi a^2$ is the toriodal magnetic flux, where B_0 the magnetic field strength at the magnetic axis. The shift is about 50% of the half-width of the crescent-shaped section, which is the approximate limit for the maintenance of good flux surfaces. We may regard the externally supplied rotational transform of 0.1 as the minimum to eliminate the requirement for central current drive.

As the transform is further increased, the plasma becomes more rigid, or robust, in the sense that even if the plasma pressure and net current suddenly disappear while the external coil currents are held fixed, as they would in a fast disruption, the magnetic surfaces remain inside the vacuum vessel. This rigidity should give a strong resilience to disruptive plasma behavior. A free-boundary equilibrium study showed that when the externally supplied rotational transform is ≈ 0.2, Figure (1.c), the plasma could be maintained with an inward shift of the magnetic axis relative to its pre-disruption state of about $0.4a$, where a is the average minor radius. When the externally provided rotational transform is greater

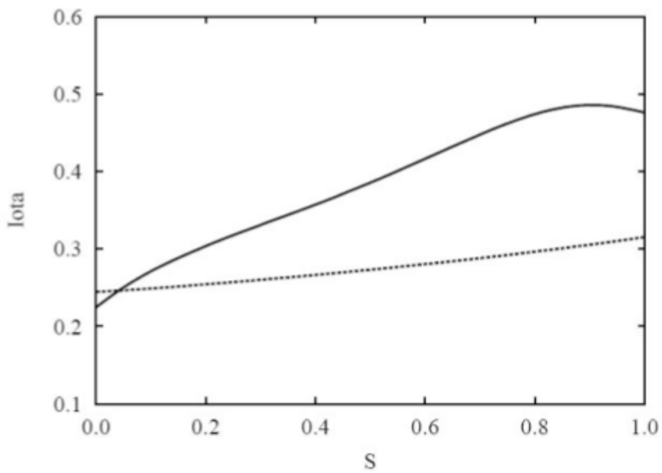

FIG. 3: Rotational transform for the plasma configuration shown in Figure (1)(d) as function of the normalized toroidal flux. The dotted line is the external transform supplied by the shaping. The solid line is the total transform including the internal contribution from the plasma current at $\beta = 4\%$.

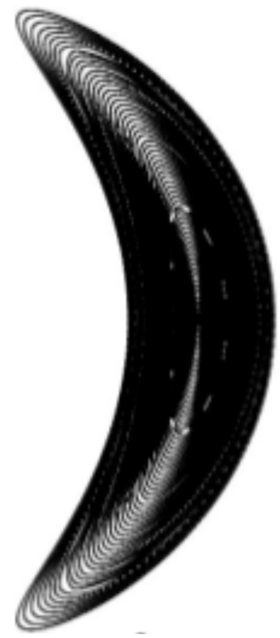

FIG. 4: Contours of flux surfaces for the configuration shown in Figure (1)(d) at $\beta = 4\%$ from a PIES calculation showing the configuration has good surface quality despite the existence of rational values in the iota profile.

than ≈ 0.2, plasmas are so rigid that little movement of the plasma is seen even for a sudden termination of the pressure and the net current. This external transform, ≈ 0.2, is slightly larger than the 0.15 that was found necessary to eliminate disruptions in the Wendelstein 7-A stellarator [26].

Within the same sequence, shaping can also be used to stabilize the kink modes, or equivalently resistive wall modes. Almost all of the configurations studied that have a vacuum transform greater than 0.1 can be stabilized, although a tradeoff with good quasi-symmetry may be necessary in some cases. The difficulty of obtaining stability depends on the location of the low order resonances and the shear in the plasma region to which the modes are most sensitive.

The final example given in Figure (1.d) is a configuration with $\iota \approx 0.3$, for which the radial profiles of the rotational transform with and without the plasma are illustrated in Figure (3). This configuration has many physics properties found in NCSX with respect to MHD stability and quasi-axisymmetry. This configuration has excellent surface quality as shown in Figure (4), which is a calculation using the PIES code [20], and is the starting point for the aspect ratio study discussed in the next section.

Figure (5) shows a distinct sequence of configurations, which have a larger external rotational transform. The external transform ranges from 0.4 to 0.6 and accounts for 75% to as much as 90% of the total transform at $\beta \approx 4\%$. These configurations have different shape from the sequence shown in Figure (1), and they also have a different shape from NCSX. They were constructed with a reduced average elongation, < 1.5, and an increased triangularity by adjusting the Δ_{20}, Δ_{-10}, and Δ_{-1-1} terms in Eq. (1). The reduced elongation helps maintain a fatter waistline at the crescent-shaped cross section when a larger amount of transform is derived from Δ_{21}, and the increased trangularity helps increase the well depth and stabilize the kink modes. These configurations have vacuum magnetic wells of $\approx 3-4\%$, which are needed to maintain the Mercier stability at high beta since the magnetic well from the plasma pressure is relatively modest due to the high rotational transform in the core. Again, the quasi-axisymmetry was targeted by ensuring the effective helical ripple, ϵ_{eff} was less than 1% in most of the plasma. These configurations are globally stable and have sufficient core transform to eliminate the need for current drive.

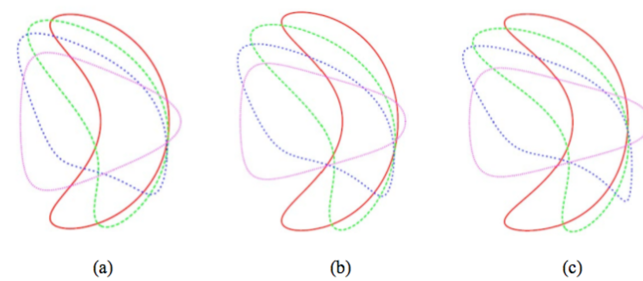

FIG. 5: Quasi-axisymmetric configurations with rotational transform provided by shaping in (a): 0.40, (b): 0.50 and (c):0.60, shown in four cross sections equally spaced in toroidal angles over half period. The vacuum transform accounts for $\approx$ 70%, 80% and 90% of the total transform at $\beta = 4\%$.

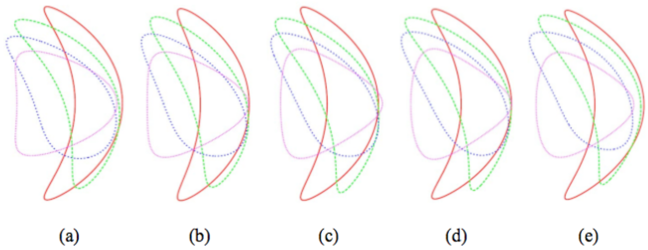

FIG. 6: Quasi-axisymmetric configurations with three periods, rotational transform from shaping ≈ 0.3 and are MHD stable to the external kink modes at $\beta = 4\%$. The aspect ratios are: (a) $A = 3$, (b) $A = 4$, (c) $A = 5$, (d) $A = 6$, and (e) $A = 8$.

IV. CONFIGURATIONS WITH THE INCREASING ASPECT RATIO

The quasi-axisymmetric sequences considered in the previous section all had an aspect ratio $A \approx 4$, which is a low aspect ratio for stellarators but has an axisymmetric tokamak with a reasonable aspect ratio as a limiting case. Stellarators of larger aspect ratios have a weaker toroidal coupling and a smaller poloidal field for a given enclosed toroidal flux and rotational transform. These features offer the potential for less complex coils. Here we demonstrate that there exist families of configurations covering a wide range of aspect ratios that meet the stability and quasi-axisymmetry targets.

Figure (6) illustrates configurations with aspect ratios A ranging from 3 to 8, all have the externally supplied rotational transform $\iota \approx 0.3$. The configuration with $A = 4$ is the same as in Figure (1)(d). The boundaries of these configurations were adjusted such that they were made stable to the external kink modes at 4% beta and have an effective helical ripple less than 1% in most of the plasma volume. We have not made effort to stabilize the ballooning modes as the unstable region at 4% is very narrow, $0.90 < r/a < 0.95$. While the unstable region is not much larger for an aspect ratio as large as 8, the growth rates do increase as A becomes larger, as seen in our calculation based on the infinite-n ballooning mode code COBRA [28]. This is consistent with ballooning theory in tokamaks, where the instability increases with A. The Shafranov shift of the magnetic axis also increases linearly with the aspect ratio. For these configurations, the rotational transform near the magnetic axis is $\iota \approx 0.25$. For $\beta = 4\%$ and $A = 8$, the shift is $\approx 21\%$ of the average minor radius a and $\approx 32\%$ of the half-width at the crescent-shaped cross section. This indicates that for $A > 10$ the shift would reach half of the narrow width so that the quality of the flux surfaces may not be adequate unless the rotational transform in the core is correspondingly increased. Figure (7) shows the shape of flux surfaces for $A = 8$ at toroidal angles corresponding to the beginning of a field period and at the half-period. For $A = 8$ and $\beta = 4\%$, the Tryon $\beta_N \equiv \beta/(I_{eff}/aB) \approx 4$, when estimated using the formula given in [8]. The effective current I_{eff} is the current that would give the poloidal field, including the field produced by the helical component. Much larger values of β_N were seen in W7AS experiments [8].

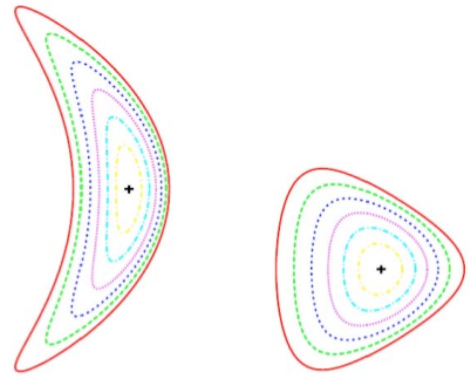

FIG. 7: Contours of flux surfaces for the configuration shown in Fig. 6 (e) with A=8 at $\beta = 4\%$ from a VMEC calculation. The Shafranov shift of the magnetic axis is about 32% of the half-width at the crescent-shaped section.

FIG. 8: Top view of modular coils constructed for configurations (b) with $A = 4$, (d) with $A = 6$, and (e) with $A = 8$ of Figure (6). Coil winding surfaces have been constructed such that the inboard midplane is displaced by $0.6a$ whereas the outboard miplane is displaced by $1.2a$, where a is the plasma minor radius, with interpolation made for locations in between. In all cases, there are three types of coils for each half-period for a total of 18 coils.

Figure (8) illustrates the effects of aspect ratio on the design of modular coils. These examples have six modular coils per field period on a winding surface which is separated from the in-board side of the plasma by $0.6a$ and from the outboard side by $1.2a$ where a is the average minor radius. As the aspect ratio increases, the toroidal excursion of the coil winding decreases, and for $A > 6$ each coil can be put in place without having interference with neighboring coils. This is a highly desirable feature in a power reactor as it eases the design for plant maintenance. The fusion power output is proportional to $B^4\beta^2R^3/A^2$, so increasing the aspect ratio to simplify a coil design comes with an obvious penalty. The device has to be bigger or the magnetic field has to be increased or β has to be increased. Ultimately, the best aspect ratio of a device would have to be determined by the over all system requirements.

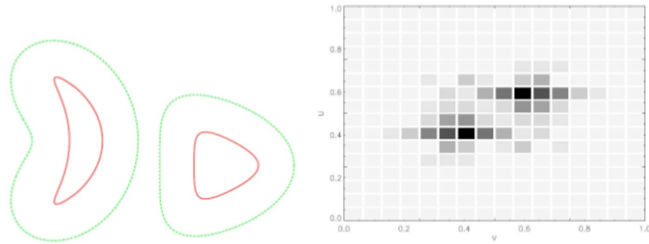

FIG. 9: Left two frames: Current carrying surface (dotted lines) relative to the plasma configuration shown in Figure (1)(d) in two cross sections. Right frame: The arrangement of the 16x16 windowpane coils wound on the current carrying surface. Currents in the windowpane coils may be controlled to produce plasma configurations (a) to (d) of Figure (1). The shading here indicates current levels for configuration (d) in linear scale, where darker shading corresponds to larger current.

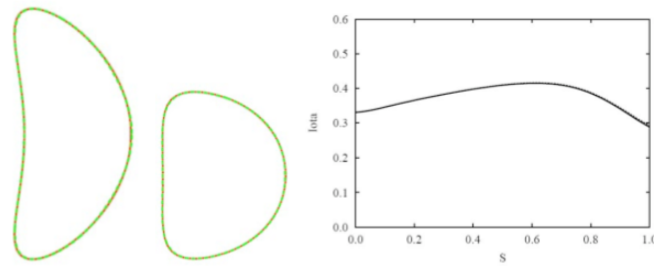

FIG. 10: Comparison of the last closed magnetic surface between the target plasma and the plasma reconstructed using the $1/R$ field and the window-pane coils whose currents are adjusted to minimize the normal field on the target boundary for the configuration with an external transform of ≈ 0.05 of Figure (1)(a), left two frames. The right frame shows the comparison of the total rotational transform, target (solid) versus reconstructed (dotted) at $\beta = 4\%$.

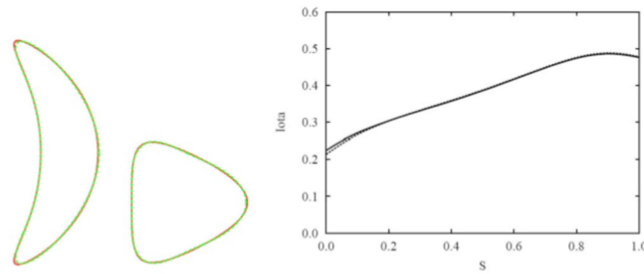

FIG. 11: Comparison of the last closed magnetic surface between the target plasma and the plasma reconstructed using the $1/R$ field and the window-pane coils whose currents are adjusted to minimize the normal field on the target boundary for the configuration with an external transform of ≈ 0.3 of Figure (1)(d), left two frames. The right frame shows the comparison of the total rotational transform, target (solid) versus reconstructed (dotted) at $\beta = 4\%$.

V. DESIGN OF A MULTI-FUNCTIONAL STELLARATOR

This section shows that it is possible to design a single set of coils to study a sequence of configurations, particularly the sequence with lower external transforms, which were discussed in Section (III) and illustrated in Figure (1). When compared to NCSX, the rotational transform of these configurations has been reduced by more than 50%. It is expected that the coils required to produce these plasmas would be simpler and more accommodating.

To generate plasmas over a range of iota and stability conditions, a combination of planar toroidal field coils and dipole-like windowpane coils were distributed on a winding surface far from the plasma. The distance of these windowpane, or trim, coils from the plasma edge is set to be the average minor radius of the plasma. In terms of the so-called coil aspect ratio, the separation is equal to the plasma aspect ratio. The windowpane coils are arranged as 16 by 16 arrays in the poloidal and the toroidal directions for each field period, Figure (9). Each coil is independently powered except as constrained by stellarator symmetry. For every case, currents in the windowpane coils were chosen to minimize the residues of the normal field on the plasma boundary. The plasmas that are constructed using these currents, along with an $1/R$ toroidal field, match very well with the target plasmas of Figure (1) from the one with the lowest external transform ≈ 0.05 to the one with the largest ≈ 0.3. Figures (10) and (11) compare the rotational transform and the plasma boundary, which has the same enclosed toroidal flux, between the originally targeted configurations and the configurations derived using the optimized coils.

Although this study used many trim coils, which would be difficult to implement, simpler designs can be obtained by optimizing the design of the coils while minimizing the normal field $\vec{B} \cdot \hat{n}$ on the plasma surface [29]. What is shown is an existence proof. It is possible to construct a single device for a range of configurations from near axisymmetry to quasi-axisymmetry with the externally supplied rotational transform exceeding 50%.

VI. SUMMARY AND CONCLUSIONS

Sequences of three-field-period quasi-axisymmetric plasmas were used in this paper to address the questions: (1) What can be achieved at various levels of non-axisymmetric shaping? (2) What simplifications to the coils can be achieved by going to a larger aspect ratio? (3) What range of shaping can be achieved in a single experimental facility?

The level of non-axisymmetric shaping was parameterized by the rotational transform produced by the shaping. The transform due to the shaping ranged from 0.05 to 0.60 and accounted for 20% to 90% of the total transform at $\beta = 4\%$. It was shown, Figure (1), that shaping can be used to: (1) stabilize the vertical mode so that the feedback control would not be needed, (2) raise the transform in the core to eliminate the need for current drive, (3) stabilize the wall modes so that a close-fitting wall and a feedback system would not be required, and (4) provide a magnetic cage stiff enough to hold the plasma within the chamber even if there were a sudden disappearance of the plasma pressure and net current. These are issues that must be addressed to achieve the programmatic mission of ITER.

Configurations were studied, Figure (6), that covered a wide range of aspect ratios, from 3 to 8, for a given rotational transform and $\beta = 4\%$. These configurations possess good quasi-axisymmetry and are also MHD stable to the external kinks. Although three dimensional shaping inevitably increases the complexity of coils, larger aspect ratio appears to simplify coil design, Figure (8). Issues such as interlocking coils and high radii of curvature complicate coil design, but are not themselves sufficient metrics of coils complexity. The development of better metrics would enable the design of better coils.

The coil designs in this study were based on a minimization of the root-mean-square of the normal magnetic field on the desired plasma boundary. No consideration was given to the relative importance of the components of the normal field on the properties of the plasma, which means the plasma sensitivity to the various possible magnetic field errors. The relative plasma sensitivity to the possible field errors is important to assess not only for coil design but also to determine the precision with which devices must be built, which is an important drive for the construction cost and schedule. In tokamaks, it is known both theoretically and experimentally that the plasma sensitivity to various perturbations differs by an order of magnitude [30]. Algorithms have been developed to include the plasma sensitivity [9] and should be implemented in future studies.

Many issues related to the three-dimensional shaping cannot be addressed by numerical studies alone. An experiment that can span a wide range of configurations can best address issues such as the minimum external transform to prevent disruptions and the effect of ϵ_{eff}, the effective helical ripple, on the actual confinement, which includes the effects of microturbulent transport. Section (V) showed that in principle a single experimental facility could explore an entire sequence of quasi-axisymmetric configurations, from a vacuum rotational transform as low as 0.05 to as high as 0.3.

The studies were carried out using available numerical tools with a reasonable degree of accuracy and completeness, but they are not exhaustive. Three field periods were used as a baseline. This makes the calculation of the stability properties for the external kinks simpler. Only two families of perturbations, the $N = 0$ and the $N = 1$ are important, and unlike the two-period case, two identical $N = 1$ modes that are toroidally displaced by 90^o are degenerate, so only one need be considered. However, a more complete study of the aspect ratio dependence of the optimization would require the consideration of two- and four-field-period configurations.

The confinement of energetic particles was not included in the studies. A small effective helical ripple ϵ_{eff} does not guarantee an acceptable loss of energetic particles. Following collisonless particle orbits to derive a loss metric is an effective way to improve stellarator configurations [15] and should be included in a more complete study of QA configurations .

Acknowledgments

This work was supported by U. S. Department of Energy through the grant ER54333 to Columbia University and the contract DE-AC02-09CH11466 to the Princeton Plasma Physics Laboratory.

[1] M. Hirsch, J. Baldzuhn, C. Beidler, R. Brakel, R. Burhenn, A. Dinklage, E. Ehmler, M. Endler, V. Erckmann, Y. Feng, J. Geiger, L. Giannone, G. Grieger, P. Grigull, H. J. Hartfuss, D. Hartmann, R. Jaenicke, R. Konig, H. P. Laqua, H. Maassberg, K. McCormick, F. Sardei, E. Speth, U. Stroth, F. Wagner, A. Weller, A. Werner, H. Wobig, and S. Zoletnik, Plasma Phys. Control. Fusion **50**, 053001 (2008).

[2] A. Komori, T. Morisaki, T. Mutoh, S. Sakakibara, Y. Takeiri. R. Kumazawa, S. Kubo, K. Ida, S. Morita, K. Narihara, T. Shimozuma, K. Tanaka, K. Y. Watanabe. H. Yamada, M. Yoshinuma, T. Akiyama, N. Ashikawa, M. Emoto, H. Funaba, M. Goto, T. Ido, K. Ikeda, S. Inagaki, M. Isobe, H. Igami, K. Itoh, O. Kaneko, K. Kawahata, T. Kobuchi, S. Masuzaki, K. Matsuoka, T. Minami, J. Miyazawa, S. Muto, Y. Nagayama, Y. Nakamura, H. Nakanishi, Y. Narushima, K. Nishimura, M. Nishiura, A. Nishizawa, N. Noda, S. Ohdachi, Y. Oka, M. Osakabe, N. Ohyabu, T. Ozaki, B. J. Peterson, A, Sagara, K. Saito, N. Tamura, K. Toi, T. Tokuzawa, K. Tsumori, T. Uda, T. Watari, I. Yamada, M. Yokoyama, Y. Yoshimura, O. Motojima, C. D. Beidler, T. Fujita, A. Isayama, Y. Sakamoto, H. Takenaga, P. Goncharov, K. Ishii, M. Sakamoto, S. Murakami, T. Notake, N. Takeuchi, S. Okajima, and M. Sasao, Fusion Science and Technology **50**, 136 (2006).

[3] M. Shimada, D.J. Campbell, V. Mukhovatov, M. Fujiwara, N. Kirneva, K. Lackner, M. Nagami, V.D. Pustovitov, N. Uckan, J. Wesley, N. Asakura, A.E. Costley, A.J.H. Donn, E.J. Doyle, A. Fasoli, C. Gormezano, Y. Gribov, O. Gruber, T.C. Hender, W. Houlberg, S. Ide, Y. Kamada, A. Leonard, B. Lipschultz, A. Loarte, K. Miyamoto, V. Mukhovatov, T.H. Osborne, A. Polevo, and A.C.C. Sips, Nuclear Fusion **47**, S1, (2007).

[4] M. Greenwald, R. Callis. D. Gates, W. Dorland, J. Harris, R. Linford, M. Mauel, K. McCarthy, D. Meade,

F. Najmabadi, W. Nevins, J. Sarff, M. Ulrickson, M. Zarnstorff, and S. Zinkle, *Priorities, Gaps and Opportunities: Towards A Long-Range Strategic Plan For Magnetic Fusion Energy*, (A Report to the U.S. Department of Energy Fusion Energy Sciences Advisory Committee, DOE/SC-0102, October 2007 available at www.science.doe.gov/ofes/FESAC_Planning_Report.pdf).

[5] V. Mukhovatov, M. Shimada, K. Lackner, D.J. Campbell, N.A. Uckan, J.C. Wesley, T.C. Hender, B. Lipschultz, A. Loarte, R.D. Stambaugh, R.J. Goldston, Y. Shimomura, M. Fujiwara, M. Nagami, V.D. Pustovitov, H. Zohm, ITPA CC Members, ITPA Topical Group Chairs and Co-Chairs and the ITER International Team, Nuclear Fusion **47**, S404 (2007).

[6] A. Weller, S. Sakakibara, K. Y. Watanabe, K. Toi, J. Geiger, M. C. Zarnstorff, S. R. Hudson, A. Reiman, A. Werner, C. Nührenberg, C. Ohdachi, Y. Suzuki, and H. Yamada, Fusion Sci. Technol. **50**, 158 (2006).

[7] M. Greenwald, Plasma Phys. Control. Fusion **44** R27 (2002).

[8] A Weller, J Geiger, A Werner, M C Zarnstorff, C Nhrenberg, E Sallander, J Baldzuhn, R Brakel, R Burhenn, A Dinklage, E Fredrickson, F Gadelmeier, L Giannone, P Grigull, D Hartmann, R Jaenicke, S Klose, J P Knauer, A Knies, Ya I Kolesnichenko, H P Laqua, V V Lutsenko, K McCormick, D Monticello, M Osakabe, E Pasch, A Reiman, N Rust, D A Spong, F Wagner, Yu V Yakovenko, W7-AS Team and NBI-Group, Plasma Phys. and Control. Fusion **45**, A285 (2003).

[9] A. Boozer, Phys. Plasmas **16**, 058102 (2009).

[10] A. Boozer, Plasma Phys. Control. Fusion **50**, 124005 (2008).

[11] J. M. Canik, D. T. Anderson, F. S. B. Anderson, C. Clark, K. M. Likin, J. N. Talmadge JN, and K. Zhai, Phys. Plasmas **14**, 056107 (2007).

[12] J. Nuhrenberg and R. Zille, Phys. Lett. A **129**, 113 (1988).

[13] P. R. Garabedian, Phys.Plasmas **3**, 2483 (1996).

[14] P. R. Garabedian and L. P. Ku, Phys. Plasmas 6, 645 (1999).

[15] L. P. Ku, P. R. Garabedin, J. Lyon, A. Turnbull, A. Grossman, T. K. Mau, M. Zarnstorff and ARIES Team, Fusion Science and Technology **54**, 673 (2008).

[16] M. C. Zarnstorff, L. A. Berry, A. Brooks, E. Fredrickson, G. Y. Fu, S. Hirshman, S. udson, L. P. Ku, E. Lazarus, D. Mikkelsen, D. Monticello, G. H. Neilson, N. Pomphrey, A. Reiman, D. Spong, D. Strickler, A. Boozer, W. A. Cooper, R. Goldston, R. Hatcher, M. Isaev, C. Kessel, J. Lewandowski, J. F. Lyon, P. Merkel, H. Mynick, B. E. Nelson, C. Nuehrenberg, M. Redi, W. Reiersen, P. Rutherford, R. Sanchez, J. Schmidt, and R. B. White, Plasma Phys. Controlled Fusion **43**, A237 (2001).

[17] F. Bauer, O. Betancourt and P. Garabedian, Magnetohydrodynamic Equilibrium and Stability of Stellarators, Springer-Verlag, New York (1984).

[18] L. P. Ku and P. Garabedian, Fusion Science and Technology **50**, 207 (2006).

[19] S. P. Hirshman, W. I. Van Rij, and P. Merkel, Comput. Phys. Commun. **43**, 143 (1986).

[20] D. Anderson, W. A. Cooper, R. Gruber, S. Merazzi, and U. Schwenn, Scient. Comput. Supercomput. II, 159 (1990).

[21] V. V. Nemov, S. V. Kasilov, W. Kernbichler and M. F. Heyn. Phys. Plasma, **6**, 4622 (1999).

[22] A. Boozer, Phys. Fluids 24, 1999(1981).

[23] P. Merkel, Nucl. Fusion 27, 867 (1987).

[24] A. Reiman, L. P. Ku, D. Monticello, S. Hirshman, S. Hudson, C. Kessel, E. Lazarus, D. Mikkelsen, M. Zarnstorff, L. A. Berry, A. Boozer, A. Brooks, W. A. Cooper, M. Drevlak, E. Fredrickson, G. Fu, R. Goldston, R. Hatcher, M. Isaev, C. Jun, S. Knowlton, J. Lewandowski, Z. Lin, J. F. Lyon, P. Merkel, M. Mikhailov, W. Miner, H. Mynick, G. Neilson, B. E. Nelson, C. Nuehrenberg, N. Pomphrey, M. Redi, W. Reiersen, P. Rutherford, R. Sanchez, J. Schmidt, D. Spong, D. Strickler, A. Subbotin, P. Valanju, and R. White, Phys Plasmas **8**, 2083 (2001).

[25] G. Y. Fu, Phys. Plasmas **7**, 1079 (2000).

[26] W7-A Team, Nucl. Fusion **20**, 1093 (1980).

[27] A. Reiman and H. Greenside, Comput. Phys. Commun. **43**, 157 (1986).

[28] R. Sanchez, S. P. Hirshman, J. C. Whitson, A. s. Ware, J. Comput. Phys. **161**, 576 (2000).

[29] D. J. Strickler, L. A. Berry, s. P. Hirshman, J. F. Lyon, D. A. Spong, D. E. Williamson, M. C. Zarnstorff, L. P. Ku, A. Brooks, S. R. Hudson, D. A. Monticello, G. H. Neilson, N. Pomphrey, A. H. Reiman, A. S. Ware, 2002 Proc. 19th Fusion Energy Conf., Lyon, France, October 2002, International Atomic Energy Agency, paper FT/P2-06.

[30] J-K Park, M. J. Schaffer, J. E. Menard, and A. H. Boozer, Phys. Rev. Lett. **99**, 195003 (2007).

The Princeton Plasma Physics Laboratory is operated
by Princeton University under contract
with the U.S. Department of Energy.

Information Services
Princeton Plasma Physics Laboratory
P.O. Box 451
Princeton, NJ 08543

Phone: 609-243-2750
Fax: 609-243-2751
e-mail: pppl_info@pppl.gov
Internet Address: http://www.pppl.gov